

Article

Experimental Investigation of the Ti-Nb-Sn Isothermal Section at 1173 K

Jianli Wang ^{1,2,*}, Libin Liu ², Ligang Zhang ², Biyang Tuo ³, Weimin Bai ² and Di Wu ²¹ School of Metallurgical Engineering, Hunan University of Technology, Zhuzhou 412007, China² School of Material Science and Engineering, Central South University, Changsha 410083, China; lbliu@csu.edu.cn (L.L.); ligangzhang@csu.edu.cn (L.Z.); tianqituo@163.com (W.B.); yntby1979@163.com (D.W.)³ College of Mining, Guizhou University, Guiyang 550025, China; yntby@163.com

* Correspondence: whwangjianli@163.com; Tel./Fax: +086-0731-2218-3469

Academic Editor: Hugo F. Lopez

Received: 21 January 2016; Accepted: 7 March 2016; Published: 11 March 2016

Abstract: Isothermal section of Ti-Nb-Sn at 1173 K was experimentally studied by back-scattered electron, electron probe microanalysis and X-ray diffraction analysis. Solid solution phase β (Ti, Nb), liquid Sn and eight intermetallic compounds Ti_3Sn , Ti_2Sn , Ti_5Sn_3 , Ti_6Sn_5 , Nb_6Sn_5 , Nb_3Sn , $\text{Ti}_3\text{Nb}_2\text{Sn}_2$ and Ti_3NbSn coexisted. Four ternary phase regions $\text{Ti}_3\text{Sn} + \text{Ti}_3\text{NbSn} + \beta$ (Ti, Nb), $\text{Ti}_3\text{NbSn} + \text{Ti}_3\text{Nb}_3\text{Sn}_2 + \text{Ti}_3\text{Sn}$, $\text{Ti}_2\text{Sn} + \text{Ti}_3\text{Sn} + \text{Ti}_3\text{Nb}_3\text{Sn}_2$ and $\text{Ti}_6\text{Sn}_5 + \text{Ti}_3\text{Nb}_3\text{Sn}_2 + \text{Nb}_3\text{Sn}$ were experimented. In addition, the proper composition range of the single phase was suggested. All the detected Ti-Sn and Nb-Sn compounds have a remarkable solubility along the isoconcentration of Sn. β (Ti, Nb) has a relatively large solution while liquid Sn has a little in the isothermal section.

Keywords: isothermal section; Ti-Nb-Sn ternary system; phase equilibrium

1. Introduction

Titanium alloys have characteristics of high strength, super-elasticity and good biocompatibility. They are promising materials in many fields especially in a biomedical aspect. Nb and Sn are alloy elements of biocompatibility, and do not increase the martensitic transformation temperature of metastable β titanium alloys [1–6]. It is necessary to know the phase equilibrium in Ti-Nb-Sn ternary system. Therefore, the knowledge of the phase diagram is of great importance in the design and development of titanium alloys.

The information of Ti-Sn, Nb-Sn and Ti-Nb binary systems can be easily found in recent studies. Ti-Sn has been systematically studied [7–14]. The version of Ti-Sn system (Figure 1a) as given by Yin *et al.* was taken because the coordinates of eutectic $L \leftrightarrow (\beta\text{-Ti}) + \text{Ti}_3\text{Sn}$ correspond better to the version of the system presented in these studies. It is also suggested that the thermodynamic model agrees well with the experimental phase diagram [10]. There are nine phases: liquid, β -Ti (bcc), α -Ti (hcp), β -Sn (bct), α -Sn, Ti_3Sn , Ti_2Sn , Ti_5Sn_3 and Ti_6Sn_5 . The composition range of solution phase β -Ti and α -Ti in Ti-Sn system is 0–7.5 at. % Sn and 0–17.0 at. % Sn, respectively. The solid solubility of Sn in Ti_3Sn and Ti_2Sn is 23.0–25.0 at. % and 32.7–35.9 at. %, respectively. In addition, Ti_6Sn_5 has two crystal structures: orthorhombic α - Ti_6Sn_5 and hexagonal β - Ti_6Sn_5 , the later one being found when the temperature was higher than 943 K [8,9].

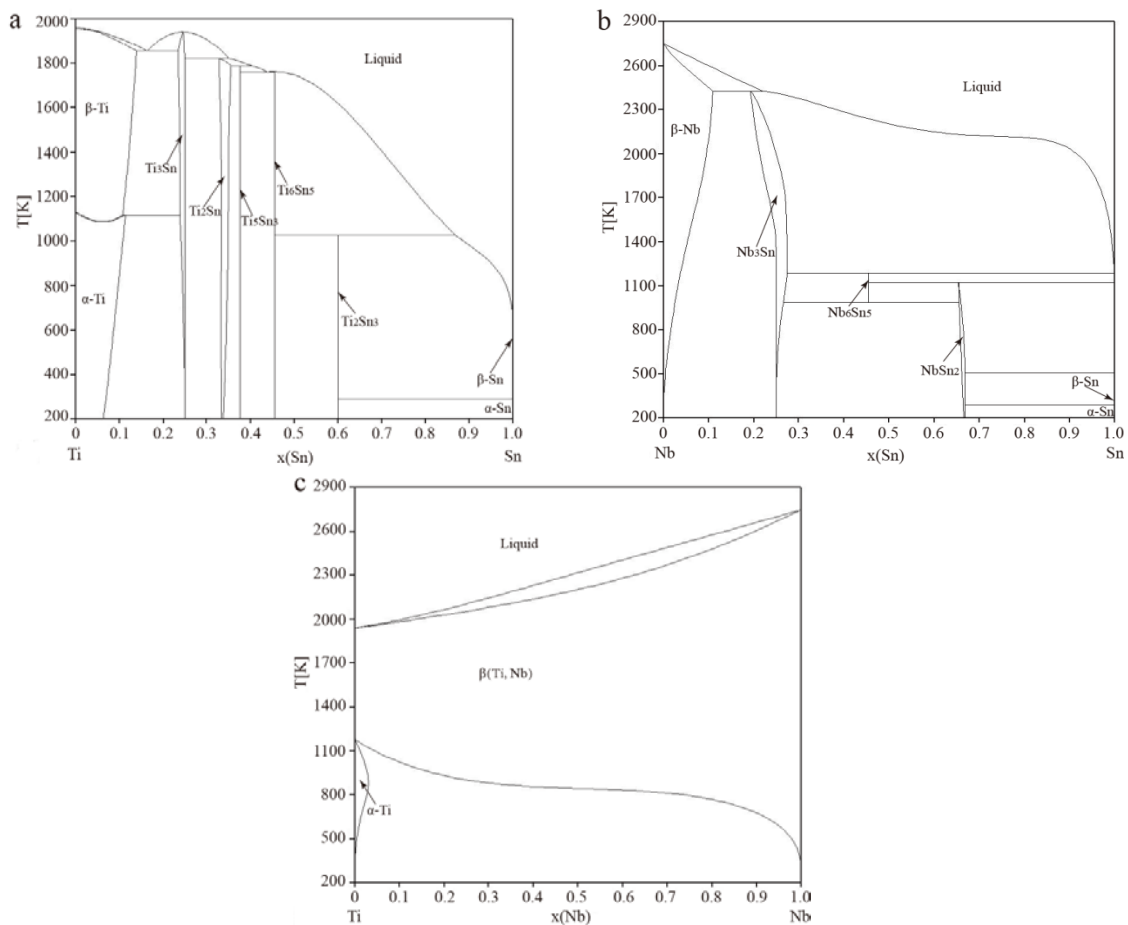


Figure 1. The binary phase diagrams: (a) Ti-Sn; (b) Nb-Sn; (c) Ti-Nb.

The Nb-Sn phase diagram was assessed by Toffolon *et al.* in 1998 [15], and the compound Nb_3Sn is assumed to be unstable below 1069 K. The system was reassessed by Toffolon *et al.* in 2001 [16] by taking the experimental enthalpy of Nb_3Sn at 1623 K into account, as well as the stability of Nb_3Sn at room temperature. Toffolon *et al.*'s reassessment agrees well with the experiment results [16]. Later, NbSn_2 was re-optimized by Li *et al.* using two sublattice model to treat the homogeneity range of NbSn_2 in Cu-Nb-Sn system based on Toffolon *et al.*'s reassessed work. The Nb-Sn phase diagram in the work (Figure 1b) is from Toffolon *et al.*'s reassessed work, for the good thermodynamic description fitting in some ternary system [16]. Three solution phases: liquid, $\beta\text{-Nb}$ and $\beta\text{-Sn}$ as well as three intermediate compounds: Nb_3Sn , Nb_6Sn_5 and NbSn_2 exist in it. The solubility of Nb_3Sn and Nb_2Sn is 19.2–26.7 at. % Sn and 65.3–66.7 at. % Sn, respectively, and compound Nb_6Sn_5 is a stoichiometric compound. The Ti-Nb phase diagram (Figure 1c) comes from the model proposed by Zhang *et al.* [17], and the thermodynamic description agrees well with the experimental results. It contains three stable phases: liquid, $\beta(\text{Ti, Nb})$ and $\alpha\text{-Ti}$.

According to the previous work [18], the Ti-Nb-Sn system has been investigated at 973 K below 50 at. % Sn. Ternary compound $\text{Ti}_3\text{Nb}_3\text{Sn}_2$ was found in the isothermal section at 973 K. It was also reported in some literatures [19–21]. The crystal structure is same to Nb_3Sn [22]. Meanwhile, the crystal structure data of phases in the Ti-Sn, Nb-Sn and Ti-Nb can be found in [14,22–24]. The purpose of this work is to evaluate the phase relations and compositions of Ti-Nb-Sn at 1173 K by means of the equilibrated alloy method (experimental assessment of two-phase and three-phase equilibria). Based on the phase diagram information, the relation of microstructure, processing and mechanical properties of titanium alloys can better understood.

2. Experimental Details

Twenty three Ti-Nb-Sn alloys were studied to evaluate the phase diagram of the ternary system. Each sample was prepared to have the weight of 6 g by pure Ti of 99.99 wt. %, Nb of 99.98 wt. % and Sn of 99.999 wt. %. They were melted in an arc furnace with nonconsumable tungsten electrode on a water-cooled copper platform in an Ar atmosphere purified by Ti-melted. The buttons were returned no less than four times to reach the homogeneity in the melting process. The specimens were encapsulated in clean quartz tubes under an argon atmosphere to prevent oxidation and other contaminations at high temperature. The 23 alloys were annealed at 1173 K for 1440 h to reach the phase equilibrium and quenched in cold water.

The samples were examined by X-ray powder diffraction (XRD, Dmax-2500VB, Rigaku Corporation, Tokyo, Japan), scanning electron microscopy (SEM Philips PSEM-500, FEI, Hillsboro, OR, USA) and electron probe microanalysis (EPMA, JXA-8230, JEOL, Tokyo, Japan). Before XRD tests, the samples were milled to less than 250 meshes in an agate mortar. XRD measurements were obtained through the Dmax-2500VB, using Bragg-Brehtano geometry, with Cu K α radiation.

The quantitative element analysis was carried out by EPMA JXA-8230 at a voltage of 20 kV and a current of 20 nA. The specimens for quantitative analysis were polished with diamond paste until scratches disappeared.

3. Results and Discussion

Twenty three Ti-Nb-Sn alloys were prepared to determine the isothermal section of Ti-Nb-Sn system at 1173 K. All phases found in the two-phase and three-phase equilibrium alloys and their compositions determined by SEM and EPMA are summarized in Table 1. In addition, most of the constituent phases are further confirmed by XRD patterns.

Table 1. Compositions of the equilibrium phases in multiphase alloys.

Alloy	Compositions (at. %)	Phase	Compositions (at. %)		
			Ti	Nb	Sn
1	Ti _{83.6} Nb _{11.3} Sn _{5.1}	β (Ti, Nb)	83.7	11.3	5.0
2	Ti _{76.6} Nb _{19.6} Sn _{3.8}	β (Ti, Nb)	76.5	19.6	3.9
3	Ti _{3.4} Nb _{95.1} Sn _{1.5}	β (Ti, Nb)	3.4	95.1	1.5
4	Ti _{75.7} Nb _{11.2} Sn _{13.1}	Ti ₃ Sn	73.3	4.3	22.4
		β (Ti, Nb)	76.9	14.5	8.6
5	Ti _{62.2} Nb _{23.5} Sn _{14.3}	Ti ₃ NbSn	59.0	20.8	20.2
		β (Ti, Nb)	65.8	26.5	7.7
6	Ti _{55.2} Nb _{31.6} Sn _{13.2}	Ti ₃ NbSn	53.8	26.8	19.4
		β (Ti, Nb)	57.0	36.8	6.2
7	Ti _{39.2} Nb _{52.1} Sn _{8.7}	Ti ₃ Nb ₃ Sn ₂	45.0	32.9	22.1
		β (Ti, Nb)	36.7	60.3	3.0
8	Ti _{27.5} Nb _{67.8} Sn _{4.7}	Ti ₃ Nb ₃ Sn ₂	35.3	43.2	21.5
		β (Ti, Nb)	26.7	70.3	3.0
9	Ti _{18.4} Nb _{69.1} Sn _{12.5}	Nb ₃ Sn	21.7	56.6	21.7
		β (Ti, Nb)	15.8	79.5	4.7
10	Ti _{9.3} Nb _{80.6} Sn _{10.1}	Nb ₃ Sn	10.9	66.8	22.23
		β (Ti, Nb)	8.2	89.1	2.7
11	Ti _{58.9} Nb _{19.7} Sn _{21.4}	Ti ₃ Sn	67.8	8.5	23.7
		Ti ₃ NbSn	54.3	25.6	20.1
12	Ti _{26.7} Nb _{49.6} Sn _{23.7}	Ti ₃ Nb ₃ Sn ₂	35.3	40.2	24.5
		Nb ₃ Sn	35.4	22.5	42.1
13	Ti _{23.3} Nb _{53.2} Sn _{23.5}	Ti ₂ Sn	62.0	4.3	33.7
		Ti ₃ Sn	68.6	5.9	25.5
14	Ti _{50.9} Nb _{6.2} Sn _{42.9}	Ti ₆ Sn ₅	49.0	5.4	45.6
		Ti ₂ Sn	55.7	8.7	35.6

Table 1. Cont.

Alloy	Compositions (at. %)	Phase	Compositions (at. %)		
			Ti	Nb	Sn
15	Ti _{42.2} Nb _{19.2} Sn _{38.6}	Ti ₆ Sn ₅	43.9	11.1	45.0
		Ti ₃ Nb ₃ Sn ₂	39.0	35.1	25.9
16	Ti _{7.5} Nb _{50.1} Sn _{42.4}	Nb ₆ Sn ₅	7.3	47.7	45.0
		Nb ₃ Sn	8.1	66.4	25.5
17	Ti _{32.0} Nb _{17.3} Sn _{50.7}	Liquid Sn	0.3	0.6	99.1
		Ti ₆ Sn ₅	35.8	19.3	45.0
18	Ti _{61.5} Nb _{19.7} Sn _{18.8}	Ti ₃ Sn	71.5	6.4	22.1
		Ti ₃ NbSn	59.7	20.2	20.2
		β(Ti, Nb)	68.0	24.0	8.0
19	Ti _{54.2} Nb _{23.9} Sn _{21.9}	Ti ₃ NbSn	51.6	28.5	19.9
		Ti ₃ Nb ₃ Sn ₂	47.8	30.34	21.9
		Ti ₃ Sn	66.2	9.1	24.7
20	Ti _{50.6} Nb _{17.9} Sn _{31.5}	Ti ₂ Sn	51.7	12.2	36.1
		Ti ₃ Sn	61.4	13.5	25.1
		Ti ₃ Nb ₃ Sn ₂	43.2	31.6	25.2
21	Ti _{50.7} Nb _{21.1} Sn _{28.2}	Ti ₂ Sn	51.7	12.2	36.1
		Ti ₃ Sn	61.4	13.5	25.1
		Ti ₃ Nb ₃ Sn ₂	43.2	31.6	25.2
22	Ti _{46.8} Nb _{24.8} Sn _{28.4}	Ti ₂ Sn	51.7	12.2	36.1
		Ti ₃ Sn	61.4	13.5	25.1
		Ti ₃ Nb ₃ Sn ₂	43.2	31.6	25.2
23	Ti _{32.3} Nb _{37.1} Sn _{30.6}	Ti ₆ Sn ₅	39.3	15.2	45.5
		Ti ₃ Nb ₃ Sn ₂	36.6	36.8	26.6
		Nb ₃ Sn	24.9	49.9	25.2

Figure 2a shows the microstructure of Alloy 12 (Ti_{26.7}Nb_{49.6}Sn_{23.7}). A gray phase with some crack phase Ti₃Nb₃Sn₂ and bright matrix phase Nb₃Sn are observed. The results are confirmed with the XRD diffractogram of Alloy 12 in Figure 3a. Figure 2b is the microstructure of Alloy 16 (Ti_{7.5}Nb_{50.1}Sn_{42.4}). Following similar analytical procedures, two phases coexisted: a gray solidification phase Nb₃Sn and gray matrix phase Nb₆Sn₅. The results agree with the XRD diffractogram of alloy 16 in Figure 3b.

Figure 2c is the microstructure of Alloy 17 (Ti_{32.0}Nb_{17.3}Sn_{50.7}). It displays a bright gray phase liquid Sn with some holes and the gray matrix phase Ti₆Sn₅ coexisted. It agrees with the XRD patterns of alloy 17 in Figure 3c.

Figure 2d–g features the microstructure of three phase region alloys. Figure 2d is the microstructure of Alloy 18 (Ti_{61.5}Nb_{19.7}Sn_{18.8}). Two precipitates dark gray phase Ti₃Sn and gray stripy phase β(Ti, Nb), as well as a bright gray matrix phase Ti₃NbSn were observed. Figure 2e shows the microstructure of Alloy 19 (Ti_{50.7}Nb_{21.1}Sn_{28.2}). There are two solidification phases, gray reticular phase Ti₃NbSn and black gray stripy phase, as well as bright gray matrix phase Ti₃Nb₃Sn₂ coexisted in the alloy.

Figure 2f shows the microstructure of Alloy 20 (Ti_{50.6}Nb_{17.9}Sn_{31.5}), which displays two precipitates containing dark gray stripy phase Ti₃Sn and bright gray reticular phase Ti₂Sn, as well as a gray matrix phase Ti₃Nb₃Sn₂ observed. Meanwhile, the XRD diffractogram of Alloy 20 is identical in Figure 3d. Compared with Alloy 19, Alloy 20 contains two same phases, but the size of solidification phases is small and slender. The size of the solidification phase is related to the content of the phase in the annealed alloy at 1173 K, while, the shape is determined by the crystal structure of phase.

Figure 2g is the microstructure of Alloy 23 (Ti_{32.3}Nb_{37.1}Sn_{30.6}). A little blocky dark gray phase Ti₃Nb₃Sn₂, bright reticular phase Ti₆Sn₅ and a gray matrix phase Nb₃Sn are observed. The result is consistent with the XRD diffractogram of Alloy 23 in Figure 3e.

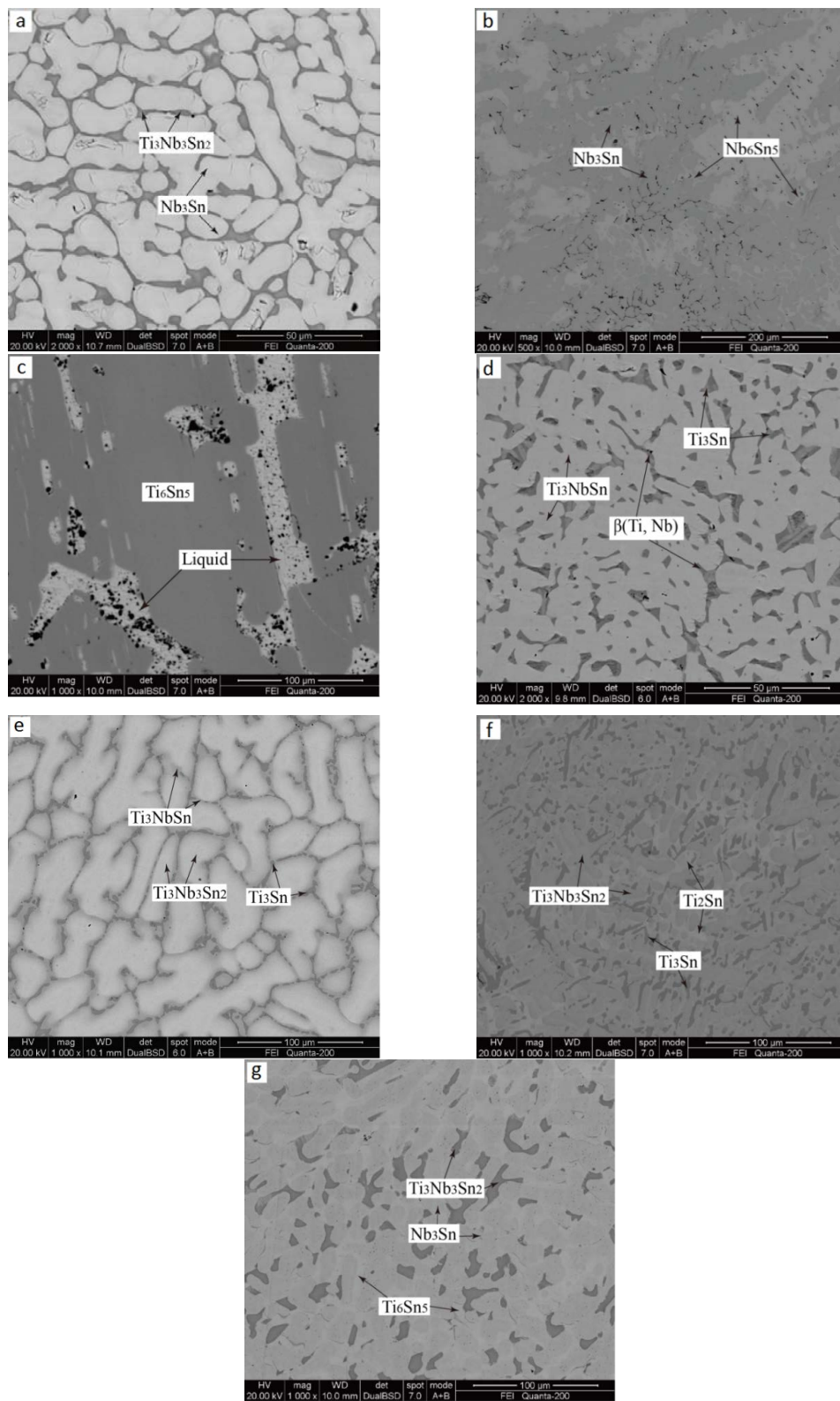


Figure 2. Microstructure of the typical alloys in Ti-Nb-Sn system annealed at 1173K for 1440 h. (a) Alloy 12; (b) Alloy 16; (c) Alloy 17; (d) Alloy 18; (e) Alloy 19; (f) Alloy 20; (g) Alloy 23.

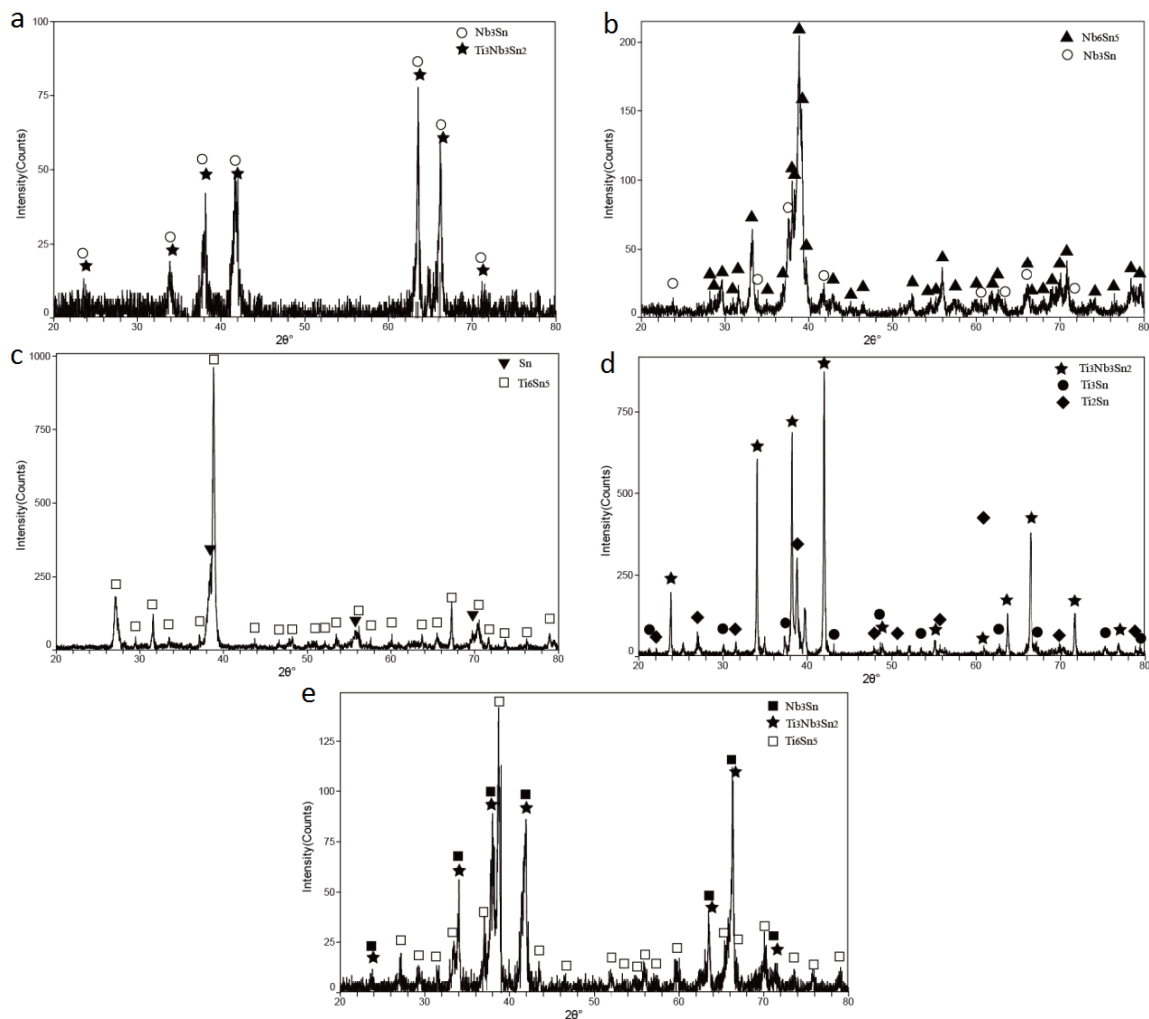


Figure 3. The XRD patterns of typical alloys in Ti-Nb-Sn system annealed at 1173 K for 1440 h. (a) Alloy 12; (b) Alloy 16; (c) Alloy 17; (d) Alloy 20; (e) Alloy 23.

The solubility of the equilibrium phases in the Ti-Nb-Sn ternary system at 1173 K is elucidated based on experimental analysis. The phase boundaries along the Ti-Sn, Ti-Nb and Nb-Sn sides can be obtained from the binary phase diagrams. In addition, the solubility of the equilibrium phases in Ti-Sn, Ti-Nb and Nb-Sn binary at 1173 K systems also given as follows. The solubility of Sn in β (Ti), Ti_3Sn , Ti_2Sn and liquid Sn in Ti-Sn system is 0–11.1 at. %, 23.8–25.0 at. %, 33.3–34.9 at. % and 79.2–100.0 at. %, respectively. The solubility of Sn in β (Nb), Nb_3Sn and liquid Sn is 0.0–3.7 at. %, 25.0–27.4 at. % and 99.8–100.0 at. %, respectively. The compounds Ti_5Sn_3 , Ti_6Sn_5 and Nb_6Sn_5 are regarded as stoichiometric compounds. The equilibrium phase in Ti-Nb at 1173 K contains only one solid solution phase β (Ti, Nb).

The solubility of Sn in β (Ti, Nb) solid solution phase can be determined by compositions of the equilibrium phases of the typical annealed alloys, and the maximum value is 3.7–11.1 at. %, which is a relative large solubility. Liquid Sn is located at the Sn rich side, and the boundary composition range is 79.2–0.2 at. % Sn from Ti side to Nb side, based on Alloy 17 and Ti-Sn and Nb-Sn binary phase diagrams, which is a smaller solubility.

The solubility of Ti_3Sn is found to be 22.1–25.5 at. % Sn and 0.0–13.6 at. % Nb. The solubility of Ti_2Sn extended along the isoconcentration of Sn, which is about 33.3–36.1 at. % Sn and more than 12.2 at. % Nb. Binary compounds Ti_6Sn_5 and Nb_6Sn_5 are treated as stoichiometric compounds for the very narrow homogeneity range according to experimental results, and the solubility extent of the

two compounds are along the isoconcentration of Sn. The maximum solubility of Ti_6Sn_5 , Nb_6Sn_5 was found to be no less than 19.3 at. % Nb and 7.4 at. % Ti, respectively, according to the equilibrium phase compositions of alloys 16 and 17. The solubility of Nb_3Sn is measured to be about 0.0–24.9 at. % Ti and 21.7–27.4 at. % Sn. The solubility of Nb in compound Ti_5Sn_3 can be deduced to be no more than 7.9 at. % Nb, based on equilibrium phase of Alloy 16. Overall, all of the detected binary compounds has a considerable solution along isoconcentration of Sn. This indicates that a certain amount of Ti atoms are replaced by Nb atoms in Ti-Sn compounds, and some Nb atoms are substituted by Ti atoms in Nb-Sn compounds.

Two ternary compounds $\text{Ti}_3\text{Nb}_3\text{Sn}_2$ and Ti_3NbSn are found in the isothermal section. The solubility of ternary compound $\text{Ti}_3\text{Nb}_3\text{Sn}_2$ is measured to be about 21.7–43.2 at. % Nb and 21.5–26.6 at. % Sn, based on the compositions of equilibrium phase of typical alloys. The solubility of Ti_3NbSn is about 20.2–28.5 at. % Nb, which is regarded as the stoichiometric compound according to the experimental results, and the extending is along the isoconcentration of Sn.

The proposed isothermal section of Ti-Nb-Sn ternary system at 1173 K in this research was determined and is presented in Figure 4. Meanwhile, the tie-lines of the two-phase alloys by the experimental measurement were given in the isothermal section. The estimated equilibria are represented by dotted lines, which are named “tentative”, as they were not confirmed by XRD, SEM and EPMA analysis.

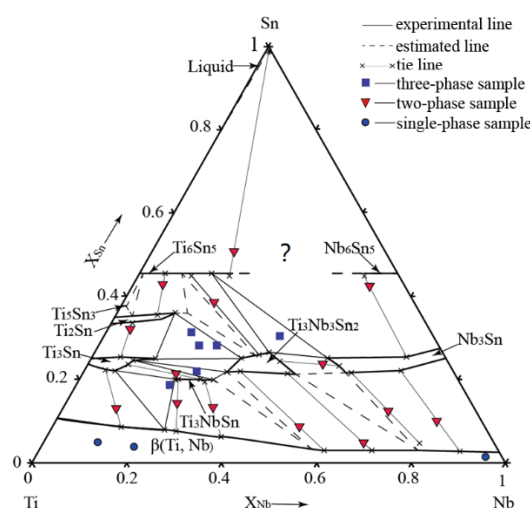


Figure 4. Isothermal section of Ti-Nb-Sn ternary system at 1173 K.

The XRD, SEM and EPMA results confirm 10 stable phases: two solution phases, six binary compounds and two ternary compounds in the isothermal section. They are $\beta(\text{Ti}, \text{Nb})$, liquid Sn, Ti_3Sn , Ti_2Sn , Ti_5Sn_3 , Ti_6Sn_5 , Nb_6Sn_5 , Nb_3Sn , $\text{Ti}_3\text{Nb}_2\text{Sn}_2$ and Ti_3NbSn . Four ternary phase fields in the isothermal section were experimentally measured, and they are $\text{Ti}_3\text{Sn} + \text{Ti}_3\text{NbSn} + \beta(\text{Ti}, \text{Nb})$, $\text{Ti}_3\text{NbSn} + \text{Ti}_3\text{Nb}_3\text{Sn}_2 + \text{Ti}_3\text{Sn}$, $\text{Ti}_2\text{Sn} + \text{Ti}_3\text{Sn} + \text{Ti}_3\text{Nb}_3\text{Sn}_2$ and $\text{Ti}_6\text{Sn}_5 + \text{Ti}_3\text{Nb}_3\text{Sn}_2 + \text{Nb}_3\text{Sn}$.

4. Conclusions

The isothermal section of Ti-Nb-Sn ternary system at 1173 K was determined by the means of equilibrated alloy method. One single phase region, 14 binary phase regions and four ternary phase regions were experimentally measured. The probable composition range of all single phases was given. The characteristic of the system is a relatively large region of the $\beta(\text{Ti}, \text{Nb})$ continuous bcc solid solution, and a small region of liquid Sn. The maximum solubility of Sn in $\beta(\text{Ti}, \text{Nb})$ is 3.7–11.1 at. %. All the detected Ti-Sn and Nb-Sn binary compounds have a remarkable solid solution in the isothermal section. This means that a certain amount of Ti atoms were replaced by Nb atoms in Ti-Sn compounds, and some Nb atoms were substituted by Ti atoms in Nb-Sn compounds. There are two ternary compounds

Ti₃Nb₃Sn₂ and Ti₃NbSn, both of which have a little solid solution. The solubility of Ti₃Nb₃Sn₂ is measured to be about 21.7–43.2 at. % Nb and 21.5–26.6 at. % Sn, and the solubility of Ti₃NbSn is about 20.2–28.5 at. % Nb.

Acknowledgments: The authors would like to thank for the financial support from the Major State Basic Development Program of China (973 Program) (No. 2014CB644000), National Natural Science Foundation of China (No. 51371200, No. 51464007), Hunan Provincial Natural Science Foundation of China (No. 14JJ3124), Natural Science Foundation of Hunan University of Technology (2013HZX20) and the Open-End Fund for the Valuable and Precision Instruments of Central South University.

Author Contributions: Jianli Wang and Libin Liu conceived and designed the equipment and experiments; Biyang Tuo, Weimin Bai and Di Wu performed the experiments; Jianli Wang and Ligang Zhang analyzed the data and wrote the report.

Conflicts of Interest: The authors declare no conflict of interest.

References

1. Banerjee, D.; Williams, J.C. Perspectives on Titanium Science and Technology. *Acta Mater.* **2013**, *61*, 844–879. [[CrossRef](#)]
2. Niinomi, M.; Kobayashi, T. Fracture Characteristics Analysis Related to the Microstructures in Titanium Alloys. *Mater. Sci. Eng. A* **1996**, *213*, 231–236. [[CrossRef](#)]
3. Hsu, H.C.; Wu, S.C.; Hsu, S.K.; Syu, J.Y.; Ho, W.F. The Structure and Mechanical Properties of As-cast Ti-25Nb-xSn Alloys for Biomedical Applications. *Mater. Sci. Eng. A* **2013**, *568*, 1–7. [[CrossRef](#)]
4. Guo, Y.; Georgarakis, K.; Yokoyama, Y.; Yavari, A.R. On the Mechanical Properties of TiNb Based Alloys. *J. Alloys Comp.* **2013**, *571*, 25–30. [[CrossRef](#)]
5. Hao, Y.L.; Li, S.J.; Sun, S.Y.; Yang, R. Effect of Zr and Sn on Young's Modulus and Superelasticity of Ti-Nb-based Alloys. *Mater. Sci. Eng. A* **2006**, *441*, 112–118. [[CrossRef](#)]
6. Gutiérrez-Moreno, J.J.; Guo, Y.; Georgarakis, K.; Yavari, A.R.; Evangelakis, G.A.; Lekka, C.E. The Role of Sn Doping in the β -type Ti-25 at. % Nb Alloys: Experiment and *ab Initio* Calculations. *J. Alloys Comp.* **2014**, *615*, 676–679. [[CrossRef](#)]
7. Murray, J.L. *Phase Diagram of Binary Titanium Alloys*; ASM International: Materials Park, OH, USA, 1987; pp. 294–299.
8. Kuper, C.; Peng, W.; Pisch, A.; Goesmann, F.; Schmid-Fetzer, R. Phase Formation and Reaction Kinetics in the System Ti-Sn. *Z. Metallkunde* **1998**, *89*, 855–862.
9. Liu, C.; Klotz, U.E.; Uggowitzer, P.J.; Löffler, J.F. Thermodynamic Assessment of the Sn-Ti System. *Monatsh. Chem.* **2005**, *136*, 1921–1930. [[CrossRef](#)]
10. Yin, F.; Tedenac, J.C.; Gascoin, F. Thermodynamic Modelling of the Ti-Sn System and Calculation of the Co-Ti-Sn System. *Calphad* **2007**, *31*, 370–379. [[CrossRef](#)]
11. Wang, J.; Liu, C.; Leinenbach, C.; Klotz, U.E.; Uggowitzer, P.J.; Löffler, J.F. Experimental Investigation and Thermodynamic Assessment of the Cu-Sn-Ti Ternary System. *Calphad* **2011**, *35*, 82–94. [[CrossRef](#)]
12. Colinet, C.; Tedenac, J.C.; Fries, S.G. Constitutional and Thermal Defects in D0₁₉-SnTi₃. *Intermetallics* **2008**, *16*, 923–932. [[CrossRef](#)]
13. Colinet, C.; Tedenac, J.C. Constitutional and Thermal Defects in B8₂-SnTi₂. *Intermetallics* **2009**, *17*, 291–304. [[CrossRef](#)]
14. Toffolon, C.; Servant, C.; Sundman, B. Thermodynamic Assessment of the Nb-Sn System. *J. Phase Equilib.* **1998**, *19*, 479–485. [[CrossRef](#)]
15. Toffolon, C.; Servant, C.; Gachon, J.C.; Sundman, B. Reassessment of the Nb-Sn System. *J. Phase Equilib.* **2002**, *23*, 134–139. [[CrossRef](#)]
16. Li, M.; Du, Z.M.; Guo, C.P.; Li, C.R. Thermodynamic Optimization of the Cu-Sn and Cu-Nb-Sn Systems. *J. Alloys Comp.* **2009**, *477*, 104–117. [[CrossRef](#)]
17. Zhang, Y.L.; Liu, H.S.; Jin, Z.P. Thermodynamic Assessment of the Nb-Ti System. *Calphad* **2001**, *25*, 305–317. [[CrossRef](#)]
18. Wang, J.L.; Liu, L.B.; Zhang, X.D.; Bai, W.M.; Chen, C.P. Isothermal Section of the Ti-Nb-Sn Ternary System at 700 °C. *J. Phase Equilib.* **2014**, *35*, 223–231. [[CrossRef](#)]

19. Watanabe, K.; Awaji, S.; Katagiri, K.; Noto, K.; Goto, K.; Sugimoto, M.; Saito, T.; Kohno, O. Highly Strengthened Multifilamentary (Nb, Ti)₃Sn Wires Stabilized with CuNb Composite. *IEEE Trans. Magn.* **1994**, *30*, 1871–1874. [[CrossRef](#)]
20. Watanabe, K.; Yamada, Y.; Sakuraba, J.; Hata, F.; Chong, C.K.; Hasebe, T.; Ishihara, M. (Nb, Ti)₃Sn Superconducting Magnet Operated at 11 K in Vacuum Using High-Tc (Bi, Pb)₂Sr₂Ca₂Cu₃O₁₀ Current Leads. *Jpn. J. Appl. Phys.* **1993**, *32*, 488–490. [[CrossRef](#)]
21. Kikuchi, A.; Taniguchi, H.; Yoshida, Y.; Tomonaga, M.; Takeuchi, T. New Ti-Sn Intermetallic Compound and (Nb, Ti)₃Sn Conductor. *IEEE Trans. Appl. Supercond.* **2009**, *19*, 2556–2559. [[CrossRef](#)]
22. Holleck, H.; Nowotny, H.; Benesovsky, F. Über das Mischungsverhalten von Nb₃Sn mit Ti₃Sn, Mo₃Al und verwandten Phasen. *Monatsh. Chem.* **1963**, *94*, 359–365. [[CrossRef](#)]
23. O'Brien, J.W.; Dunlap, R.A.; Dahn, J.R. A Mössbauer Effect and X-ray Diffraction Investigation of Ti-Sn Intermetallic Compounds: II. Nanostructured Phases Prepared by Ball Milling with Al₂O₃ and TiN. *J. Alloys Comp.* **2003**, *353*, 60–64. [[CrossRef](#)]
24. Okamoto, H. Sn-Ti (Tin-Titanium). *J. Phase Equilib. Diffus.* **2010**, *31*, 202–203. [[CrossRef](#)]



© 2016 by the authors; licensee MDPI, Basel, Switzerland. This article is an open access article distributed under the terms and conditions of the Creative Commons by Attribution (CC-BY) license (<http://creativecommons.org/licenses/by/4.0/>).